Research Article

Stress Performance Evaluation of Shield Machine Cutter Head during Cutting Piles under Masonry Structures

Fei Peng,[1,2] Shiju Ma [iD],[1] Mingyu Li,[1] and Kui Fu[3]

[1]*School of Civil Engineering, Zhengzhou University, Zhengzhou, China*
[2]*Henan Provincial Communications Planning & Design Institute Co., Ltd., Zhengzhou, China*
[3]*China Railway 18th Bureau Group First Engineering Co., Ltd., Hebei, China*

Correspondence should be addressed to Shiju Ma; mashiju2010@126.com

In the construction of the metro, the development and operation of large-scale underground space in the city cause the construction of metro tunnels near the original underground structures, and the complex environment for passing structures at close range has increased significantly. Comparing the actual load data of the actual project with the data obtained with the proposed new method, it is proved that the predicted load range corresponds essentially to the measured average curve of the project, which is commonly used with the experimental load formula. Subsequently, the load calculation method is used to guide the construction of the composite base of the protective cutting pile of one of the Zhengzhou metro lines under the existing masonry structure. Based on the existing building damage grade evaluation standards, the professional house inspection agency checked the intersection of the tunnel and the building space and realized that the main structure of the house during the tunnel construction process would be still safe; thereby, Zhenghe Community Building 1# can be used normally after partial repairs.

1. Introduction

The pile-soil composite foundation is considered as a composite soil and provides an efficient approach to shield loading when the composite foundation of the shield shear pile group penetrates the existing masonry structure. Compared with the past, recent projects are large-scale and more adjacent to underground systems, even touching underground piles. It can cause severe environmental problems of rock and soil such as tilting, cracking, and even collapse of the building. This not only affects the routine use of buildings and causes significant economic losses but also poses a serious threat to the lives and property of nearby residents. When there are buildings at the top of the tunnel, subsidence and soil deformation are different from buildings without buildings. Hence, internal and external researchers have conducted extensive research on the impact of underground tunnel construction on adjacent structures. Finno et al. in connection with theoretical/analytical explorations of the problem [1] created a new building model under reasonable and simple conditions. They used this model to study surface displacement due to shield drilling. Han et al. [2] revised the pack formula [3] and proposed a method for predicting the building sitting curve by considering the structural rigidity of the building—the stiffness correction method, but this method is only suitable for building seats with a Gaussian distribution curve. Match Ouyang et al. [4] considered the effect of building stiffness but did not consider the stiffness of the foundation. Using the principle of equivalent stiffness, the building was equivalent to a layer of soil with similar properties to the subsoil using the Verruijt and Booker solution. The calculation formula is derived for the settlement of buildings on the surface resulting from the construction of the shield. The performance of the shield device is mainly reflected by its operating parameters such as forward speed, thrust, torque, and rotation speed of the cutter head [5].

According to the measured analysis method, Shen [6] analyzed the subsidence and slope characteristics of the buildings resulting from the construction of the shield based on an engineering example of the shield section passing through a subset of buildings on Line 1 of the Chengdu

Metro. Sun and Guan [7] monitored the installation of the floor and ceiling of the building resulting from the construction of a two-lane bumper, along with the case of Hangzhou Metro Line 1 from the underpass of 13 residential complexes. It was found that the next meeting of the masonry structure, which is considered to be the ratio of the accumulated meeting, is obviously more than the natural surface meeting. Xu et al. [8] analyzed the measured data of the shield tunneling stage and studied the characteristics and rules of building deformation due to the shield tunneling. Based on typical engineering examples of six subway tunnels that pass under buildings in the Beijing city, as mentioned by Sun et al. [9], they show that the bending point of the significant impact zone of the base depression is about 0.3 to 0.6 H from the tunnel axis, and the depression law almost follows Peck's correction formula.

Given the development of a finite element method for such a problem, Milliziano et al. [10] used a 2D numerical method to analyze the impact of tunnel construction on a particular masonry structure and obtain the building subsidence curve. Peng et al. [11] used a three-dimensional numerical analysis method to calculate the building structure subsidence resulting from the construction of a two-line parallel shield tunnel. Giardina et al. [12] studied the interactions between sand-tunnel-ground structures through 3D numerical simulation and concluded that the impact of tunnel drilling on buildings is not just relative stiffness between soils and soil it depends, but it also depends on the weight of the building. Ding et al. [13] simulated the effect of shield drilling on the building stress distribution through the finite element method and proposed reinforcement measures to improve the rigidity and integrity of the building based on the finite element simulation results. Most of the above research focuses on ground subsidence resulting from the construction of shield tunnels and uneven subsidence of buildings. Quantitative analysis and research have been done on the selection of construction parameters when the shield penetrates into the masonry structure.

Here, based on the underlying structure of the composite base structure of the Zhengzhou Metro Line 5 bumper pile-cutting group, theoretical calculations are used to obtain the recommended values of construction parameters such as total thrust, total torque, and injection pressure length. Making a shield candle: along with the actual on-site measurements, the settling rules and the deformation of the masonry structure are analyzed during the construction process of shield pile-cutting piles. Finally, the theoretical results obtained with the observed data for the shield construction parameters are successfully confirmed. Successful completion of a project can certainly be a reliable source for similar works in the future.

2. Materials and Methods

2.1. Engineering Background.
Currently, research on protective structures in such layers mainly focused on construction technology innovation, excavation surface stability and configuration, and cutter and cutting headwear. [14] For the shield section of Zhengzhou Metro Line 5 with staggered

assembly construction, the geometrical data are as follows: the length of the left tunnel is 1214.457 m, the maximum longitudinal slope of the line is 26.78%, the minimum slope is 2%, and the minimum radius of curvature of the shield tunnel is 400 m, and the buried depth of the interval tunnel is in the range of 15.7 to 28.5 m. The inner and outer diameters of the segment, thickness, and width in order are 5.5, 6.2, 0.35, and 1.5 m. The concrete strength is categorized into the group C50, and the impermeability grade is P12.

The mileage of the left line of the interval section is DK13 + 662.558~DK13 + 711.322 (685~715 ring, length is about 48.764 m) obliquely crosses the 7-story masonry structure in the northwest-southeast direction, and the height is 18.8 m. The foundation adopts reinforced concrete strips, the foundation concrete is C30, there is no basement, and it was constructed in 2007. The foundation is cement deep mixing pile composite foundation Ø500@950, the pile length is 11.5 m, and the pile end extends into the bearing layer not less than 750 mm. The shield machine will cut off the cement-soil mixing pile of the original building by 2.6~3.7 m. The number of left-line shields that invaded the mixing piles was about 175, accounting for about 16% of the total piles of the masonry structure composite foundation. The thickness of the top cover of the shield tunnel's lining structure crossing the masonry structure section is 12.1 ~ 13.5 m. The geographical location of the project is shown in Figure 1.

2.2. Geological Conditions.
The principle of operation of this method is to cut the soil from the front cutter and transfer it out of the cave by transport vehicles, while the next part is done by jacks [15]. The site of the shield section belongs to the alluvial plain of the Yellow River. The layer at a depth of 30 meters of the site is mainly the Holocene Quaternary layer (Q4), and the initial layer is 0–20 meters of sand silt, clay silt, and silt clay with silt and fine sand. This layer varies from medium-dense to fine-grained sand. The tunnel structure is mainly located in the fine sand layer and the silty clay layer. The depth of cover above the tunnel is 12.1 to 13.5 meters, and the water depth above the tunnel varies in the range of 4.4 to 6.4 meters. Figure 2 shows the shield tunneling in different layers, and Table 1 shows the soil parameters.

3. Suggested Values for Construction Parameters of Shield Cut Piles

During the tunneling process, the propulsive torque provided by the multiple inverter motor is transmitted from the planetary reducer and the pinions to the gears that are permanently attached to the cutting head [16]. Under normal conditions of construction, the impedance of drilling piles to cut the shield to the ground and the composite foundation should be reduced. The main construction parameters to be determined are total thrust, total torque, injection pressure, advance speed, and cutting head speed [16].

3.1. Prediction of the Total Thrust and Total Twist.
Regardless of the load transfer effect of the pile, the composite gravity method is adopted, and the displacement
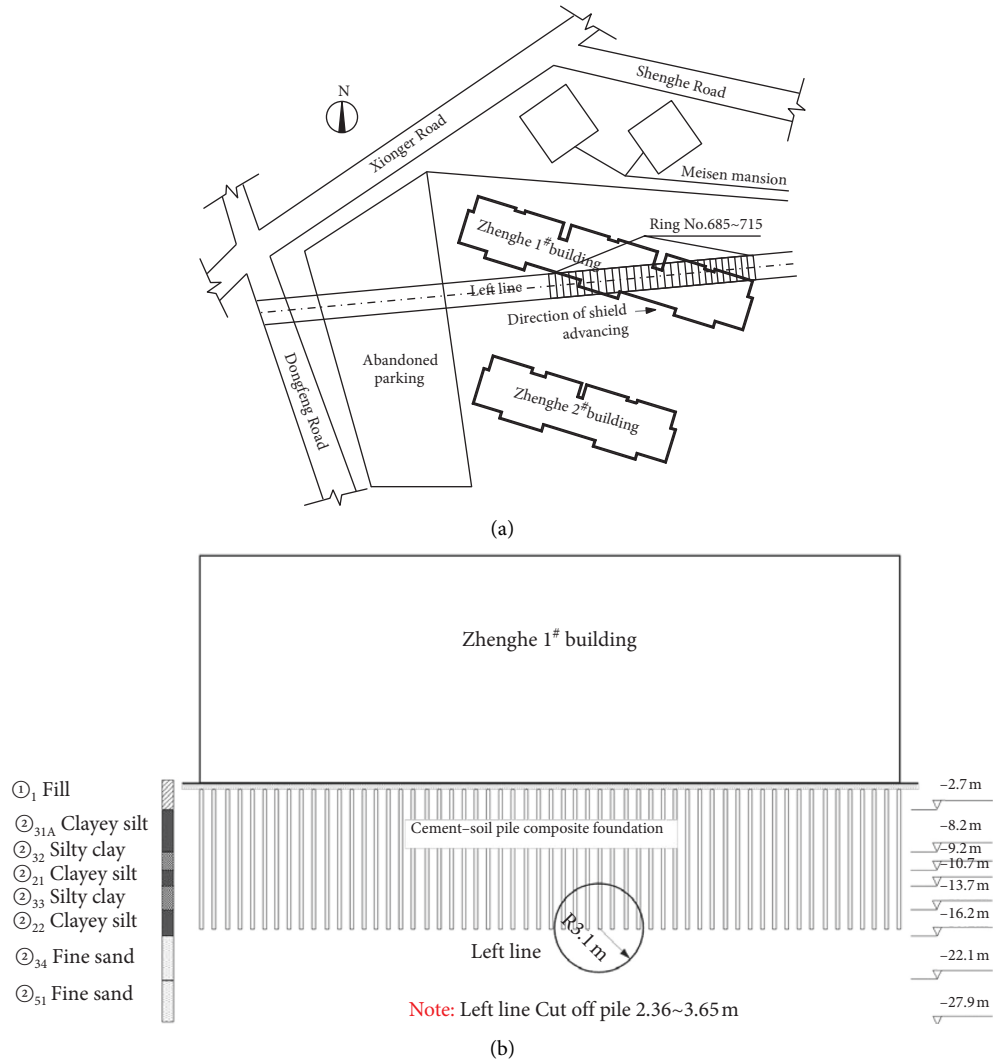
(a)

(b)

FIGURE 1: Relative position of the Zhenghe 1#: (a) schematic plane location of the tunnel and Zhenghe 1# building; (b) schematic elevation of the tunnel and Zhenghe 1# building.

effect of the pile on the soil is considered. The composite foundation reinforcement area is regarded as a composite soil body, and the gravity of the composite soil body is determined by the following equations:

$$m = \frac{\pi d^2}{4l^2} \text{ (Plane and squar layout of piles)}, \quad (1)$$

where m is the replacement rate of composite foundations (a dimensionless factor), d denotes the pile diameter in meter, and l is the pile spacing of unit meter. Further,

$$\gamma' = m\gamma_p + (1 - m)\gamma_s, \quad (2)$$

where γ'/(kN/m^3) is the weight of the composite soil; γ_p/(kN/m^3) is the weight of the pile material; and γ_s/(kN/m^3) is the weight of the natural foundation soil. The calculations performed and the results obtained are shown in Table 2 [17].

Krause [18] evaluated the construction load data of 397 Japanese and 12 German shields and proposed the following empirical calculation formulas for total thrust force and total shield torque:

$$F = \beta D^2,$$
$$T = \alpha D^3, \quad (3)$$

where F/kN is the total thrust of the shield, T/(kN·m) is the total torque, D/m is the shield's diameter, α and β are empirical coefficients whose values chiefly rely on the formation conditions, shield type, and shield structure. At present, the commonly used value ranges of the earth pressure balance shield in examining engineering problems are $\alpha = 8 \sim 23$ and $\beta = 500 \sim 1200$ [19]. It is noteworthy that the above experimental formula is strongly influenced by the diameter of the bumper machine. When the diameter of the bumper machine is small, the total thrust force and the total torque obtained will be very small, which is reflected in the insufficient thrust and cutting ability during the protective tunneling. Conversely, in the case of a larger diameter bumper machine, the bumper tunneling and drilling ability
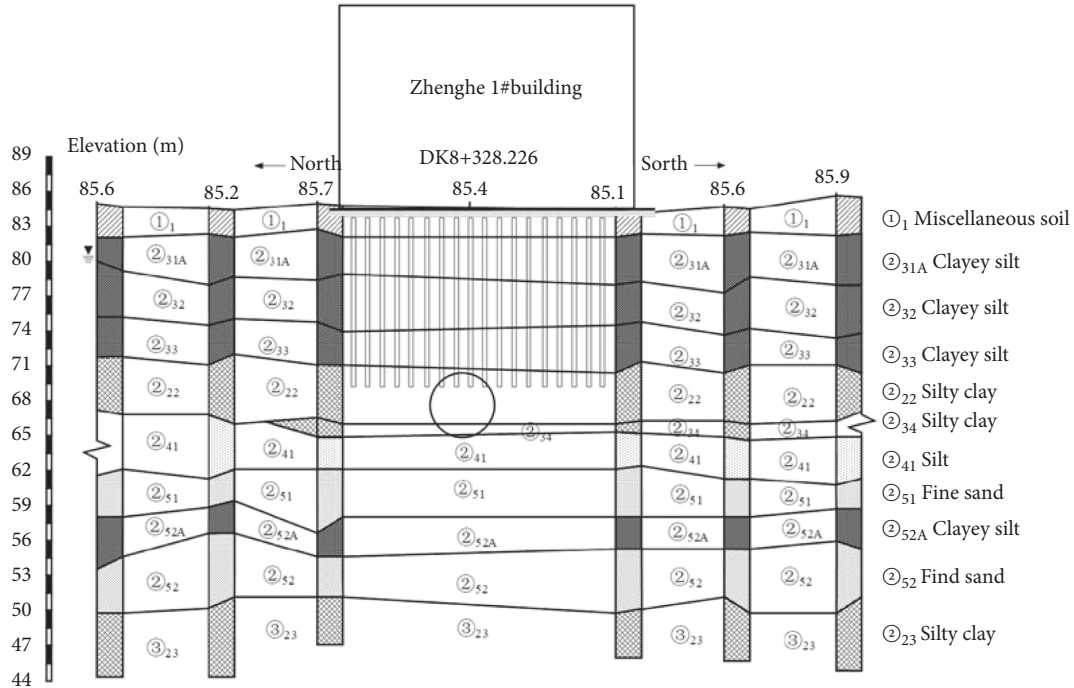
FIGURE 2: Shield crossing geological section.

TABLE 1: Parameters of soils.

Numbering	Layer	C (kPa)	φ (°)	μ	γ (kN/m³)	Thickness (m)
①₁	Fill soil	20	20	0.333	18	2.7
②₃₁ₐ	Clay silt	20	22.1	0.296	18.9	2.6
②₃₂	Clay silt	19.9	21.2	0.301	19.4	2.9
②₂₁	Silty clay	29.5	16.4	0.355	19.6	1.0
②₃₃	Clay silt	19	20.4	0.324	19.9	1.5
②₂₂	Silty clay	31.2	15.6	0.375	19.4	3.0
②₃₄	Clay silt	19.3	20.7	0.333	20.2	2.5

TABLE 2: Heaviness of the composite soil.

Soil layer number	Name	The natural weight of soil (kN/m³)	Composite soil weight (kN/m³)
①₁	Fill soil	18.0	18.4340
②₃₁ₐ	Clay silt	18.9	19.1387
②₃₂	Clay silt	19.4	19.5302
②₂₁	Silty clay	19.6	19.6868
②₃₃	Clay silt	19.9	19.9217
②₂₂	Silty clay	19.4	19.5302
②₃₄	Clay silt	20.2	20.1566

cannot be fully utilized. Based on the experimental formula, the total thrust and total torque intervals of the shield are relatively wide, and determining the best construction parameters while cutting the piles is somewhat difficult and more accurate calculations are required [5].

As shown in Figure 3, when the shield machine excavates the composite foundation pile group underground, the power system of the shield machine provides the total thrust F and the full torque T to overcome the resistance and the resistance torque during the excavation. In Figure 3, the main factors affecting the total thrust of the shield are explained in the following: F_1 is the

frictional resistance between the shield shell and the soil, F_2 is the frontal resistance of the excavation surface, and F_3 is the penetration resistance of the cutter head. The main factors affecting the total torque of the shield are as follows: T_1 is the friction torque generated by the front of the cutter head and the composite soil, T_2 is the friction torque generated by the side of the cutter head and the composite soil, and T_3 is the torque between the stirring rod and the muck in the sealed chamber, resulting in stirring torque [15]. The remaining impacts are fairly small and will not be considered in this analysis. According to the mechanical balance relationship:
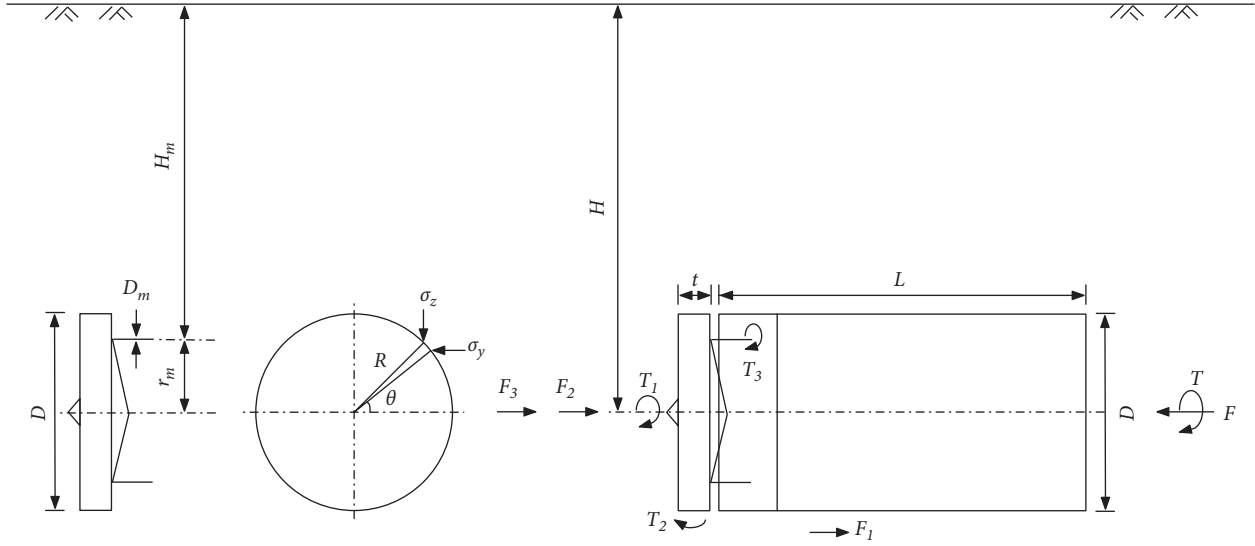
FIGURE 3: Force analysis of the shield tunneling.

$$F = F_1 + F_2 + F_3, \tag{4}$$

$$T = T_1 + T_2 + T_3. \tag{5}$$

The normal stress σ_N acting on the shield shell is as follows:

$$\sigma_N = \sigma_y \sin \theta + \sigma_z \cos \theta. \tag{6}$$

$$\sigma_z = \sum \gamma_i' h_i + P_0, \tag{7}$$

$$\sigma_x = \sigma_y = K_0 \left(\sum \gamma_i' h_i + P_0 \right), \tag{8}$$

where γ_i' and h_i in order are the gravity and thickness of ith layer of the composite soil, and p_0/kPa is the building's additional load. The latter factor is estimated according to the "Code for Loads of Building Structures" (GB50009-2012) [20]: $P_0 = 7$ (number of floors) × 18 kPa (load on each floor of residential buildings) + 20 kPa (load on basement) + 10 kPa (foundation load) = 156 kPa, and K_0 is the static lateral pressure coefficient of the soil, which can be evaluated by the semi-empirical formula $K_0 = 1 - \sin \phi$. Through multiplying equation (6) by the friction coefficient μ_1 and integrating the resulting expression over the contact area, the friction resistance F_1 between the shield shell and the composite soil is obtained as follows:

$$F_1 = 2 \int_0^L \int_0^\pi \left(\sigma_y \sin\theta + \sigma_z \cos\theta \right) \mu_1 r \, d\theta \, dl$$
$$= 4K_0 \mu_1 r \left(\sum \gamma_i' h_i + P_0 \right) L. \tag{9}$$

In (9), we assume $\mu_1 = 0.3$ [21], L/m is the length of the shield shell, and r/m is the radius of the shield machine. The frontal resistance F_2 of the excavation surface is calculated according to the static earth pressure. The frontal strength is equal to the sum of the ground pressure due to the gravity of the composite body and the additional load on the building:

$$F_2 = \int_0^{2\pi} \int_0^{\frac{D}{2}} K_0 \gamma' (H - r \sin \theta) r \, dr \, d\theta$$
$$+ K_0 P_0 = \frac{\pi D^2}{4} K_0 \gamma' H + K_0 P_0, \tag{10}$$

where H/m indicates the vertical distance between the ground and the axis of the cutter head of the bumper device. Cutter head penetration resistance, F_3, is calculated as follows:

$$F_3 = D\pi L' \left[\tan\varphi \left(\sum \gamma_i' h_i + P_0 \right) + c \right], \tag{11}$$

where L' is the length of the notched ring, and its value is estimated to be the ratio of the shield's tunneling speed to the cutter head's rotating speed. The frictional torque T_1 between the front of the cutter head and the composite soil is as follows:

$$T_1 = \int_0^{2\pi} \int_0^{\frac{D}{2}} (1 - \eta^2) K_0 \mu_2 \gamma' (H - r \sin\theta) r^2 \, dr \, d\theta (1 - \eta)^2 \frac{\pi D^3}{12} K_0 \mu_2 \gamma' H, \tag{12}$$

where μ_2 the coefficient of friction between the cutting head and the soil. Normal tension on the cutter consists of two parts: the vertical stress σ_2 and the lateral stress σ_y. Then, the friction torque (i.e., T_2) between the side of the cutter head and the composite soil can be calculated as follows:

$$T_2 = \int_0^{2\pi} r^2 \mu_2 \gamma' t (H - r \sin\theta) \sin^2 \theta \, d\theta$$
$$+ \int_0^{2\pi} r^2 \mu_2 \gamma' t K_a (H - r \sin\theta) \cos^2 \theta \, d\theta \tag{13}$$
$$= \pi r^2 (1 + K_a) \mu_2 \gamma' H t,$$

where t denotes the width of the cutter head's outer edge, and K_a is the active earth pressure coefficient. The stirring

torque (i.e., T_3) generated between the stirring rod and the residue in the sealed chamber is given as follows [21]:

$$T_3 = \sum_n \gamma' H_m D_m l_m r_m \mu_3, \tag{14}$$

where H_m/m is the vertical distance between the ground and the stirring rod, D_m and l_m are the diameter and length of the stirring rod, respectively, r_m is the distance between the stirring rod and the central axis of the shield cutter head, μ_3 is the coefficient of friction, and n is the number of stirring rods. In summary, equations (5), (9)–(11) give the theoretical calculation formula for the total thrust during the penetration of the shield cut pile group composite foundation as follows:

$$F = 2K_0 \mu_1 r \left(\sum \gamma_i' h_i + P_0 \right) L + \frac{\pi D^2}{4} K_0 \gamma' H \\ + K_0 P_0 + D\pi L' \left[\tan\varphi \left(\sum \gamma_i' h_i + P_0 \right) + c \right]. \tag{15}$$

Based on equations (5), (12), (13), and (14), the theoretical formula for the total torque would be derived as follows:

$$T = (1 - \eta) \frac{\pi D^3}{12} K_0 \mu_2 \gamma' H + \pi r^2 \left(1 + K_a \right) \mu_2 \gamma' H t \\ + \sum_n \gamma' H_m D_m l_m r_m \mu_3. \tag{16}$$

3.2. Propulsion and Cutter Head Speed. During the entire construction of the shield cut pile group composite foundation traversing the existing masonry structure, the shield advancement speed is maintained at a uniform speed, controlled within the range of 10 to 20 mm/min. Progress rates can be appropriately accelerated or reduced according to ground speed and building monitoring conditions. The speed setting range of the cutter head during pile cutting is 1.07 to 1.12 r/min.

4. Comparative Analysis of Shield Cutting Pile Cutter Head Force Calculation

The total thrust (F) and the total torque (T) of the shield are calculated using the suggested load calculation method for shield cutting pile excavation, and then, these values are compared with the actual measured values of the project. The selected pile-cutting engineering section of Zhengzhou Metro Line 5 has a total of 31 tunnels. Figures 4 and 5 show the total thrust and total torque curves predicted by the proposed calculation method and those measured by the project. Besides, the empirical formula estimates are given as load range. The comparison shows that the load range obtained based on the calculation method proposed in this study is basically the same as the measured average curve of the project. Compared with the current commonly used load empirical formula to estimate the range, the prediction accuracy has been greatly improved. In addition, as shown in Figure 6, this study calculated the proportion of each load
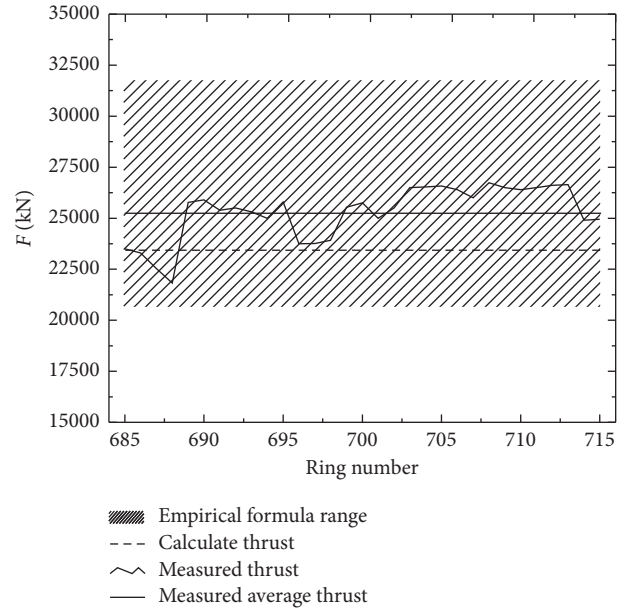

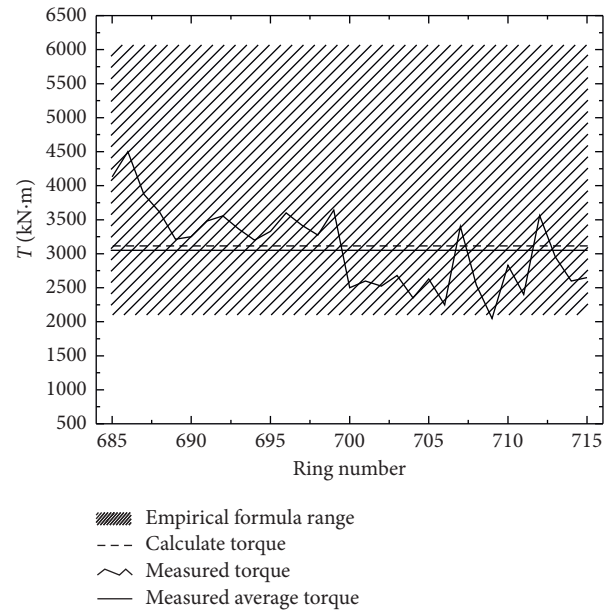FIGURE 4: Comparison of total thrust during shield cutting piles.

FIGURE 5: Comparison of total torque during shield cutting piles.

component in the total load in the project. The penetration resistance of the cutter head is 40.3% of the total drift. For the front of the cutter head and the composite soil, the friction torque makes up 81.2% of the total torque, which is the load ratio with the highest ratio.

In summary, the calculation method of cutter head load when shield cutting piles is proposed in this study can be used as a supplement to the empirical formula, providing more comprehensive and effective theoretical guidance for the current shield cutting pile construction and design. Of course, there is still a certain difference between the load calculation and the actual load. The work of this study aims to establish an effective method for determining the load
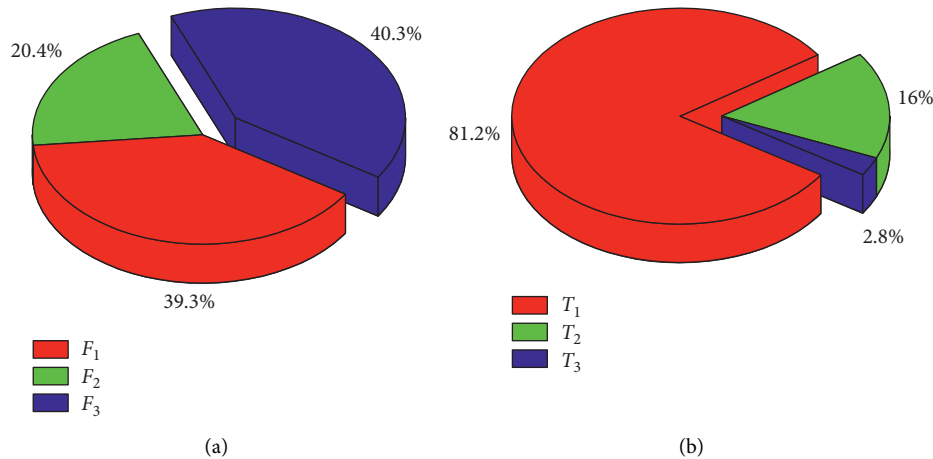
Figure 6: Percentage of various forces in the shield cutter head load.

range of shield cutting pile excavation that is convenient for engineering applications. Therefore, the pile-soil composite foundation is equivalently simplified in the calculation model, and only several main load action forms and the most critical influencing factors, in the follow-up research work, will improve and refine the calculation model in this study, to further provide prediction accuracy.

5. Building Deformation Monitoring during Shield Cutting Pile Tunneling

5.1. Monitoring Data Analysis. Under the requirements of "Urban Rail Transit Engineering Monitoring Technical Specifications" [22] and "Urban Rail Transit Engineering Measurement Specifications" [23], combined with the geological conditions of the project and the characteristics of the building, the building settlement monitoring points along the outer wall of the building are separated about 10 to 15 m. Concerning the outer wall, there should be a monitoring point control layout at the corners. The measuring points are arranged clockwise at the corners of the building, marked F1~F19 (i.e., 19 measuring points in total). The layout of the deformation monitoring points of Zhenghe 1# building is shown in Figure 7.

Prior to passing through the composite base of the cut tunnels in the bumper tunnel, # 1 building was closely monitored for deformation to fully understand the condition and safety level of # 1 building. As shown in Figure 8(a), the monitoring results show that the maximum differential subsidence between the south and north facades of the Zhenghe 1# building and the maximum distortion are 0.55 mm/m and $3.05 \times 10-3$ rad/m, respectively. Currently, in the actual measurement and analysis of the impact of shield tunnel intersection construction on existing buildings, the greatest concern of buildings is whether the cumulative assembly exceeds the control standard after the assembly has been established. The more in-depth research is only about the settlement along a particular facade of the building. However, during the shield tunnel's excavation process, there is a considerable time difference in the cutter head reaching the two facades of the building. This issue will cause

these facades' settlement to be inconsistent, producing permanent distortion of the building. This study mainly analyzes the distortion and deformation characteristics of the masonry structure caused by the underpass of the shield pile group pile composite foundation. Figures 8(b)–8(d), respectively, present the change in the settlement surface at each critical moment during the bottom plane of Zhenghe 1# building under the left-line tunnel cut pile composite foundation. Based on the sequence of tunnel construction, we select three critical moments for analysis. Figure 8(b) shows the case when the left-line shield cutter cuts into the composite foundation and starts to cut piles (indicated by time B). Figure 8(c) corresponds to when the shield's tail on the left line breaks out of the composite foundation, and the pile cutting is completed (indicated by time C). Finally, Figure 8(d) is related to the case of stabilized settlement of the building (don't use time D to indicate).

It can be observed from Figures 8 and 9 that during the whole process of the left-line cut pile composite foundation of the shield tunnel, most of the measurement points on the bottom plane of the building showed settlement. The north facade's maximum settlement was approximately the same as that of the south front, and its value is twice the maximum settlement at the intersection of the tunnel and the building space. Nevertheless, the settlement of the measurement points on the same plane is quite different, indicating the occurrence of distortion in the bottom plane, and the magnitude of the distortion is constantly changing with the shield construction process. After stabilizing the settlement, the bottom plane of the building was permanently twisted and deformed. According to Table 3 and Figures 8 and 9, the locations where the largest differential settlement and the largest distortion of the building occur are close to the central axis of the left tunnel. Among understudy critical times, the largest differential settlement for the north-south façade would be 8.42 mm/m, detectable at time C, and the maximum distortion occurs at time B, whose value is 3.376×10^{-2} rad/m. When the settlement is finally stabilized at time D, the maximum values of settlement, differential settlement, and distortion of the building's measuring point would be −10.98 mm, 8.37 mm/m, and 3.12×10^{-2} rad/m, respectively.
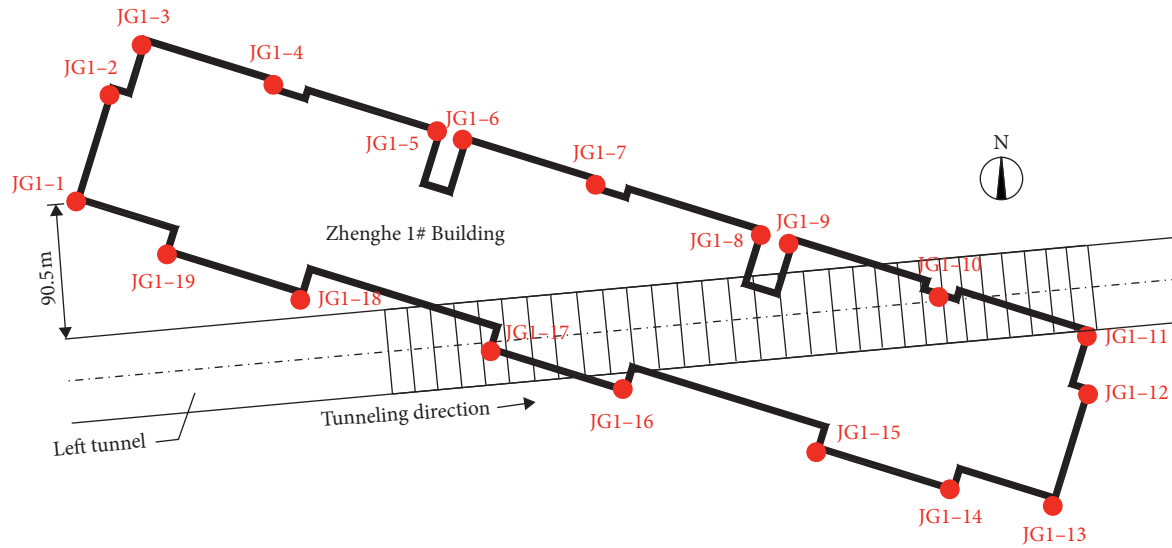
FIGURE 7: Layout drawing of the monitoring points in Zhenghe 1# building.
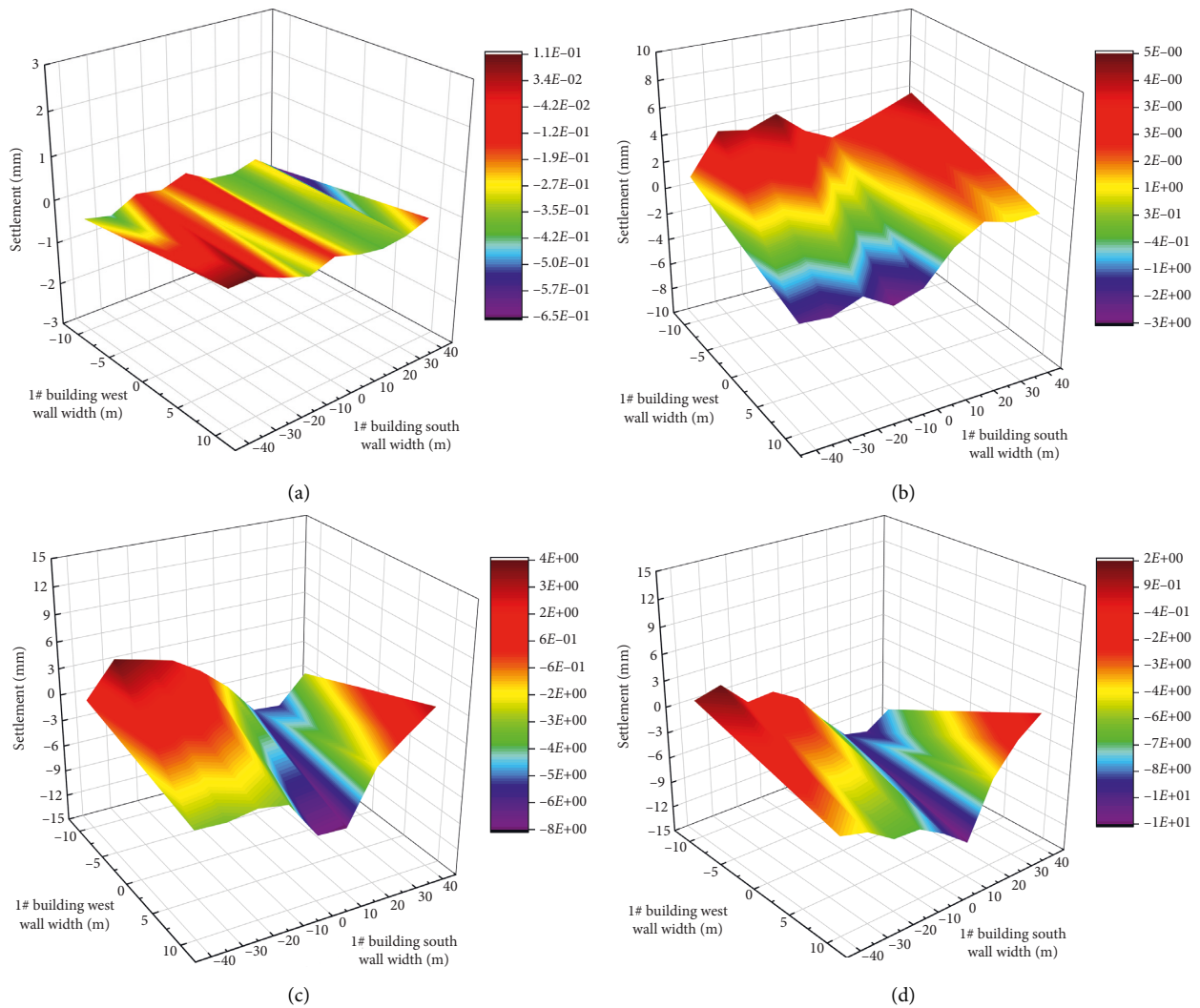

(a)

(b)

(c)

(d)

FIGURE 8: Deformation of buildings at various critical moments of shield cutting pile group construction. (a) Deformation of buildings when shield tunnels are not under construction. (b) The left-line shield cutter head starts to cut the pile group composite foundation. (c) Left-line shield tail separated from pile group composite foundation. (d) The shield tail of the left line is away from the pile group composite foundation for 15 days.
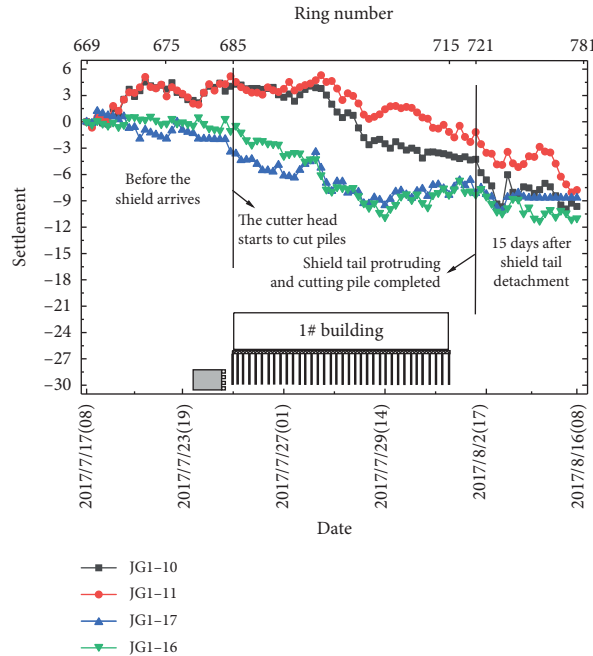
FIGURE 9: Settlement time history of the crucial measuring points in the whole process of the cut pile construction.

TABLE 3: Maximum differential settlement and maximum distortion of the building at each critical moment in the construction of shield cut group piles.

Monitoring items	Time A	Time B	Time C	Time D
Maximum differential settlement (mm/m)	7.43	8.18	8.42	8.37
Maximum distortion (rad/m)	1.65×10^{-2}	3.376×10^{-2}	3.368×10^{-2}	3.12×10^{-2}

TABLE 4: Building damage grade evaluation standard.

Risk level	Maximum slope	Differential settlement* (mm/m)	Building distortion* (rad/m)	Risk description
1	< 1/500	< 2	$< 4 \times 10^{-3}$	Ignorable: shallow damage is unlikely
2	1/500~1/200	2~5	$4 \times 10^{-3} \sim 1 \times 10^{-2}$	Minor: may be damaged in shallow parts, but has no effect on the structure
3	1/200~1/50	5~20	$10^{-2} \sim 4 \times 10^{-2}$	Moderate: shallow damage, possible structural damage, possible related rigid pipe damage
4	> 1/50	> 20	$> 4 \times 10^{-2}$	Serious: building structure damage, rigid pipeline damage, possible other pipeline damage

Note.* newly added evaluation annotations by Yang and Zhang [24].

5.2. Zhenghe 1# Safety Evaluation Based on Existing Deformation.

According to the judgment criteria of Yang and Zhang [24] based on the scrutiny of Rankin [25], the proposed damage grade correction evaluation standard considering both differential settlement and distortion of the building has been provided in Table 4. The damage degree of Zhenghe 1# building before the shield tunnel is negligible, and the risk level would be equal to 1. According to Table 3, the maximum differential settlement of the north and south facades of Zhenghe 1# building at each moment is less than 10 mm/m, and the maximum distortion value of the building is less than 4×10^{-2} rad/m. On the other hand, the maximum values of distortion and differential settlement of the building are also less than 5% of their maximum allowable values.

According to the building damage grade evaluation mark given in Table 4, after the shield cutting pile group composite foundation is penetrated, the damage degree of Zhenghe 1# building is medium, and the risk grade would be 3. Since the largest differential settlement and the largest distortion are located at the diagonal intersection of the tunnel and the building, the corresponding location of Zhenghe 1# building should be tested to see whether necessary reinforcement and repair measures are required. After examination by a professional house inspection agency, it was found that the main structure of the house is still safe during the tunnel construction process. Further, the 1# building of Zhenghe Community meets the normal standards of the building usage and can be utilized normally after partial repair.

6. Conclusions

From the engineering point of view, a comprehensive analysis of the cutter head force during cutting the piles by the shield machine is carried out. To this end, the pile-soil composite foundation is equivalently simplified into a composite soil body, and the calculation formula for the cutter head load when the shield machine cuts the composite foundation pile group is given. Based on the above method, the comparison of the total load of the cut pile group under the masonry structure of Zhengzhou Metro Line 5 with the actual measured value is performed and it is observed that the suggested method can effectively predict both total thrust and torque during the excavation of the shield pile group. The load calculation method in this study is used to guide the construction of the shield-bored cut pile composite foundation of Zhengzhou Metro Line 5 through the existing masonry structure. By monitoring the deformation of Zhenghe 1# building, the final maximum differential settlement of the north and south facades of the building and the maximum distortion are 8.42 mm and 3.376×10^{-2} rad/m. Analysis of monitoring data shows that the differential assembly and the distortion of the masonry structure are in the safe range.

Data Availability

The data used to support the findings of this study are available from the corresponding author upon request.

Conflicts of Interest

The authors declare that they have no conflicts of interest.

Acknowledgments

References

[1] R. J. Finno, F. T. Voss, E. Rossow, and J. T. Blackburn, "Evaluating damage potential in buildings affected by excavations," *Journal of Geotechnical and Geoenvironmental Engineering*, vol. 131, no. 10, pp. 1199–1210, 2005.

[2] X. Han, J. R. Standing, and N. Li, "Stiffness correction method for prediction of building deformation caused by tunnel construction," *Journal of Geotechnical Engineering*, vol. 31, no. 4, pp. 539–545, 2009, in Chinese.

[3] R. B. Peck, "Deep excavations and tunneling in soft ground," in *Proceedings of the 7th Int. Conf. Soil Mech. & Found. Eng., Mexico, State of the Art*, pp. 225–290, Maxico, USA, 1969.

[4] W. B. Ouyang, Q. W. Ding, and D. W. Xie, "Calculation method of settlement caused by shield construction considering building stiffness," *Chinese Journal of Underground Space and Engineering*, vol. 9, no. 1, pp. 155–166, 2013, in Chinese.

[5] C. Wan and Z. Jin, "Adaptability of the cutter-head of the earth pressure balance (epb) shield machine in water-rich sandy and cobble strata: a case study," *Advances in Civil Engineering*, vol. 2020, Article ID 8847982, 12 pages, 2020.

[6] J. Y. Shen, "Analysis of the impact of shield tunneling of Chengdu metro line 1 on building safety," *Modern Tunnel Technology*, vol. 45, no. 2, pp. 63–68, 2008, in Chinese.

[7] Y. K. Sun and F. L. Guan, "Impact of shield tunneling on settlement of masonry structures," *China Railway Science*, vol. 33, no. 4, pp. 38–44, 2012, (in Chinese).

[8] Z. M. Xu, Q. H. Han, and G. Zheng, "Measurement and analysis of the influence of metro tunnels passing through historical building," *Chinese Journal of Geotechnical Engineering*, vol. 35, no. 2, pp. 354–364, 2013, in Chinese.

[9] X. Y. Sun, C. Y. Heng, and Z. Zhou, "Field measurement of the induced settlement of the foundation of Beijing subway tunnels through masonry structures," *Journal of Civil Engineering*, vol. 1, no. S2, pp. 304–308, 2015, in Chinese.

[10] S. Miliziano, F. M. Soccodato, and A. Burghignoli, "Evaluation of damage in masonry buildings due to tunneling in clayey soils," in *Proceedings of the 3th Int. Conf. Geotechnical engineering technology for soft soil base*, pp. 49–54, Lyon, France, 2002.

[11] C. Peng, Y. L. Ji, and H. B. Luo, "Numerical simulation of influence of double-line shield construction on adjacent buildings," vol. 27, no. S2, pp. 3868–3874, 2008, in Chinese.

[12] G. Giardina, M. J. Dejong, and R. J. Mair, "Interaction between surface structures and tunnelling in sand: centrifuge and computational modelling," *Tunnelling and Underground Space Technology*, vol. 50, pp. 465–478, 2015.

[13] L. Ding, X. Wu, L. Zhang, and M. J. Skibniewski, "How to protect historical buildings against tunnel-induced damage: a case study in China," *Journal of Cultural Heritage*, vol. 16, no. 6, pp. 904–911, 2015.

[14] F. Ye, N. Qin, X. Gao, X.-yong Quan, X.-zhuo Qin, and B. Dai, "Shield equipment optimization and construction control technology in water-rich and sandy cobble stratum: a case study of the First Yellow river metro tunnel undercrossing," *Advances in Civil Engineering*, 8358013, vol. 2019, 12 pages, 2019.

[15] Y. Zhu, J. Wang, B. Zhang, X. Zhang, and J. Zhu, "Research studies on the thrust of special-shaped full-sectional cutterheads of quasirectangular shield," *Advances in Civil Engineering*, vol. 2021, Article ID 8830512, 12 pages, 2021.

[16] W. Sun, H. Ma, X. Song, L. Wang, and X. Ding, "Modeling and dynamic analysis of cutterhead driving system in tunnel boring machine," *Shock and Vibration*, vol. 2017, Article ID 7156816, 12 pages, 2017.

[17] X. Zou, H. Zheng, and Y. Mi, "Performance evaluation of hard rock TBMs considering operational and rock conditions," *Shock and Vibration*, vol. 2018, Article ID 8798232, 17 pages, 2018.

[18] B. Maidl, M. Herrenknecht, and L. Anheuser, *Mechanized Shield tunneling*, Ernst & Sohn, Berlin, Germany, 1996.

[19] W. Zhu, *Standard Specification for Tunnels (Shield Tunnel) and Explanation*, China Construction Industry Press, Beijing, China, 2001.

[20] Ministry of housing and urban-rural development of the people's Republic of China, *Building Structure Load Code" (GB50009-2012)*, Building Industry Press, Beijing, China, 2012.

[21] Q. Lv and D. M. Fu, "Simulation test research on torque of earth pressure balance shield tunnel boring machine cutter-

head," *Chinese Journal of Rock Mechanics and Engineering*, vol. 25, no. S1, pp. 3137–3143, 2006, in Chinese.

[22] Ministry of housing and urban-rural development of the people's Republic of China, *Technical Specifications for Urban Rail Transit Engineering Monitoring" (GB50911-2013)*, Building Industry Press, Beijing, China, 2013.

[23] Ministry of housing and urban-rural development of the people's Republic of China, *Urban Rail Transit Engineering Survey Specification"(GB50308-2008)*, Building Industry Press, Beijing, China, 2008.

[24] Y. Y. Yang and Z. X. Zhang, *Shield Tunnel Construction Disaster Mechanism and Engineering practice*, China Building Industry Press, Beijing, China, 2014.

[25] W. J. Rankin, "Ground movements resulting from urban tunnelling: predictions and effects," *Geological Society, London, Engineering Geology Special Publications*, vol. 5, no. 1, pp. 79–92, 1988.